International Journal of Nanomedicine

Dovepress
Taylor & Francis Group

Open Access Full Text Article

REVIEW

How Key in vivo Models Can Advance Anticancer Nanotherapeutics

Gudapureddy Radha[1], B Devika Chithrani[1,2]

[1]Department of Physics and Astronomy, University of Victoria, Victoria, BC, V8P 5C2, Canada; [2]Centre for Advanced Materials and Related Technologies (CAMTEC), University of Victoria, Victoria, BC, V8P 5C2, Canada

Correspondence: B Devika Chithrani, Department of Physics and Astronomy, Centre for Advanced Materials and Related Technologies (CAMTEC), University of Victoria, Victoria, BC, V8P 5C2, Canada, Email devikac@uvic.ca

Abstract: Nanomedicine offers powerful opportunities for targeted drug delivery and cancer therapy, yet clinical translation remains limited by the complex and dynamic interactions of nanoparticles within biological systems. This review integrates current evidence on how nanoparticle size, shape, and surface properties govern cellular uptake and processing, systemic biodistribution, immune interactions, and therapeutic performance across in vitro, ex vivo, and in vivo models. By comparatively analyzing findings across two-dimensional, three-dimensional, xenograft, and immunocompetent tumor models, this review identifies model-dependent determinants of nanoparticle performance that influence translational outcomes. Foundational studies in two-dimensional monolayers established relationships between physicochemical attributes, endocytic pathways, vesicular trafficking, and exocytosis. Three-dimensional spheroids introduce extracellular matrix density and cellular packing constraints that limit nanoparticle movement and alter uptake trends observed in monolayers. In vivo, xenograft models emphasize the influence of vascular permeability and stromal architecture but often overestimate delivery due to exaggerated enhanced permeability and retention effects and the lack of adaptive immunity. Immunocompetent tumor models capture complement activation, opsonization, macrophage-mediated clearance, dynamic protein corona evolution, and cytokine-driven vascular changes. These immune-mediated processes reshape biodistribution patterns and often diminish ligand-mediated targeting benefits. They operate alongside systemic factors such as renal and hepatosplenic filtration, biotransformation, and species-specific differences in vascular structure and immune composition, influencing nanoparticle pharmacokinetics and therapeutic response. Together, these findings underscore that successful nanomedicine design requires integrating material engineering with an understanding of immune surveillance, vascular biology, tumor microenvironment heterogeneity, and whole-body transport dynamics. Future progress will depend on developing nanoparticles that maintain functional stability in immune-intact hosts, minimize premature clearance, and achieve sustained intratumoral delivery. These advances must be supported by predictive, physiologically relevant models that bridge gaps between in vitro results, preclinical outcomes, and clinical translation.

Keywords: nanoformulations, 2D cultures, 3D spheroids, immunocompetent model, tumor microenvironment, biodistribution

Introduction: Nanoparticle Design and Biological Barriers in Cancer Nanomedicine

Nanomedicine has emerged as a powerful approach in cancer treatment, enabling selective drug delivery, enhanced imaging, and improved therapeutic outcomes.[1] Unlike conventional small molecule drugs that diffuse passively and cause systemic toxicity, nanoparticles (NP) can be engineered to achieve targeted accumulation at tumor sites and provide sustained release of therapeutic agents, thereby improving both efficacy and safety.[2,3] These NP-based systems, collectively termed nanoformulations, include examples such as liposomes, polymeric micelles, dendrimers, and metal-organic frameworks.[4–6] In addition to serving as drug carriers, NP can be functionalized with therapeutic ligands, peptides, or surface chemistries that exert direct anticancer activity by inducing oxidative stress, disrupting cellular membranes, or enhancing radiation sensitivity.[7,8] This multifunctional design allows NP to act simultaneously as delivery vehicles and active therapeutic agents, broadening their potential in combinatorial cancer therapy. Clinically approved examples include liposomal doxorubicin (Doxil),[9,10] in which the anthracycline drug doxorubicin is enclosed within

https://doi.org/10.2147/IJN.S558763
Received: 30 December 2025
Accepted: 24 March 2026
Published: 11 April 2026

Graphical Abstract

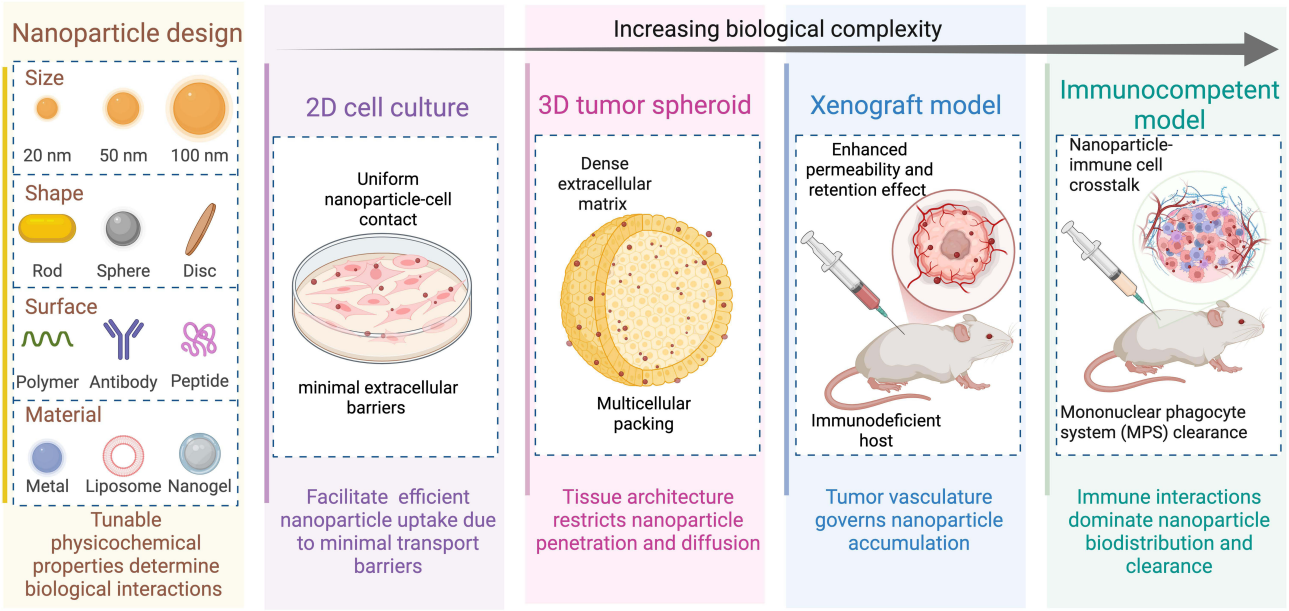

a lipid bilayer vesicle, and albumin-bound paclitaxel (Abraxane),[10,11] where paclitaxel is conjugated to nanosized albumin complexes. Despite these advances, translation of nanomedicine to the clinic remains limited by challenges such as poor intratumoral penetration, rapid systemic and immune-mediated clearance, variable patient-specific responses, and complex, often unpredictable interactions within the biological milieu.[12–14] These limitations highlight the need for a deeper mechanistic understanding of NP-cell interactions and the physicochemical factors governing their intracellular fate.

NPs vary widely in composition and structure, including metallic, lipid-based, polymeric, hydrogel, and hybrid systems, each offering tunable characteristics such as size, shape, and surface chemistry.[2,4] Many metal-based, polymeric, and hydrogel NP can be synthesized in diverse geometries including spheres, rods, discs, and polygonal forms.[15–18] Lipid-based systems such as liposomes and micelles, primarily assemble into spherical structures but still allow broad size control.[19,20] Size and shape tuning is often achieved by adjusting synthesis variables such as precursor concentration, reaction temperature, nucleation rate, and surfactant or stabilizer ratios, while specialized templates or growth-directing additives enable non-spherical geometries.[21] These structural and dimensional variations dictate how NP engage the plasma membrane, activate distinct endocytic pathways, and localize within intracellular compartments.[22] Surface chemistry further defines charge, hydrophobicity, and reactivity. Through surface modification, NP properties can be tailored to influence biological interactions. For example, polyethylene glycol (PEG) coatings enable NP to avoid immune recognition to a certain extent,[23,24] while ligand conjugation with molecules such as transferrin, folic acid, or arginine-glycine-aspartic acid (RGD) peptides enables selective binding to receptors overexpressed on cancer cells.[25,26] Collectively, these physicochemical parameters govern how NP are internalized, retained, and cleared from biological systems.[13]

Intracellular fate encompasses the complete journey of NP once they contact a cell, including uptake, trafficking through endosomes or lysosomes, exocytosis, and retention.[28,29] Each stage is affected by the particle's physicochemical properties. Cellular uptake occurs through both passive and active mechanisms. Very small or neutrally charged NP may cross the plasma membrane by direct translocation or limited passive diffusion and diffuse more freely within the cytoplasm, whereas larger, positively charged, or negatively charged NPs typically rely on energy-dependent endocytic

pathways that require membrane remodelling and are more likely to remain confined within endosomal or lysosomal vesicles.[30,31] These include clathrin-mediated endocytosis, caveolae-mediated endocytosis, macropinocytosis, and receptor-mediated endocytosis, where ligand-functionalized NP engage specific surface receptors.[30,32] After internalization, NP progress through early and late endosomes and are subsequently directed either to lysosomes for degradation, released into the cytosol, or routed back to the plasma membrane through recycling pathways. Exocytosis and recycling ultimately govern intracellular retention time.[33] Understanding these interconnected processes is vital for improving therapeutic selectivity and minimizing off-target effects.

Despite major advances in vitro, NP often fail to reproduce similar outcomes in vivo. This discrepancy stems from the complexity of the tumor microenvironment, which contains dense extracellular matrices, irregular vasculature, and hypoxic gradients.[34,35] Two-dimensional (2D) cultures facilitate NP uptake uniformly, while three-dimensional (3D) spheroids and tumors impose diffusion barriers that restrict penetration and retention.[36] Additionally, plasma proteins adsorb onto NP surfaces to form a dynamic protein corona, altering biological identity and triggering immune clearance.[37,38] Typically less than one percent of the injected dose reaches the tumor, underscoring the need for predictive models that better recapitulate in vivo barriers.[39] These observations emphasize that early cellular studies capture only a fraction of the biological challenges NPs encounter after systemic administration. A key challenge is understanding how NP design principles translate into effective performance within immune-competent tumor environments, where systemic clearance and immune surveillance often outweigh cellular uptake mechanisms. Although ligand and peptide functionalization enhances receptor-specific uptake in controlled in vitro systems, many targeting strategies lose efficacy in vivo. Surface-displayed peptides are susceptible to proteolytic degradation and structural instability, reducing functional ligand density and limiting sustained receptor engagement before tumor accumulation.[40,41] Protein corona formation can mask targeting ligands and accelerate immune-mediated clearance.[42] Linear L-amino acid peptides are particularly prone to rapid enzymatic degradation in circulation. D-amino acid substitution and mirror-image ligand strategies improve protease resistance and in vivo stability.[41] In contrast, monoclonal antibodies exhibit greater structural stability and long systemic half-lives, and several antibody-based targeting strategies have achieved clinical success due to their high affinity and favorable pharmacokinetics.[43] These comparisons underscore that effective NP targeting requires not only receptor specificity but also biochemical stability and sustained functionality within immune-competent biological environments.

Bridging this gap requires integrating advanced material design with physiologically relevant models. Three-dimensional spheroids and animal systems now provide more realistic insights into NP-cell interactions, effectively linking in vitro findings with in vivo outcomes.[44] Nearly a decade after the seminal work of Chithrani et al revealed quantitative evidence of size-dependent endocytosis, the field has evolved toward a multiscale understanding that connects NP properties with therapeutic efficacy.[27,45] The current focus of researchers is on designing NPs capable of navigating complex tumor microenvironments while minimizing premature clearance, and achieving sustained intracellular retention. Importantly, immune surveillance and protein corona evolution are central regulators of NP behaviour, linking material design to biodistribution and therapeutic response.[46]

A comprehensive understanding of how NP physicochemical properties influence intracellular fate is essential for optimizing their use in drug delivery, diagnostics, and therapy. The following sections review how variations in NP dimensions, geometry, and surface characteristics regulate cellular uptake and processing, integrating evidence from quantitative 2D studies and extending through 3D spheroid and in vivo cancer models.

This article was prepared as a structured narrative review of the literature. Relevant studies were identified through searches of PubMed, Google Scholar, and Web of Science using keywords related to NP size, shape, surface chemistry, intracellular fate, biodistribution, and tumor models. The review focuses primarily on peer-reviewed articles published between 2005 and 2025. Foundational mechanistic studies and recent translational investigations were prioritized to provide a balanced comparison of NP behavior across in vitro, xenograft, and immunocompetent models.

How in vitro Models Help Understand NP Uptake and Intracellular Fate

2D Monolayer Cell Cultures

The influence of NP size on cellular internalization was established through systematic 2D culture studies that identified an optimal size range for maximum uptake. The pioneering work by Chithrani et al quantified citrate-stabilized spherical gold NPs in HeLa (Henrietta Lacks) cells across 14–100 nm and identified 50 nm as the most efficiently internalized size (Figure 1A).[27] In a follow-up study, the same group examined size-dependent uptake and exocytosis using transferrin-coated gold NPs.[45] These particles entered cells through clathrin-mediated endocytosis, where smaller NPs (<50 nm) required clustering of multiple receptors to initiate membrane curvature, and larger NPs (>50 nm) internalized more slowly due to extended membrane wrapping times. Exocytosis followed an inverse size trend, with smaller NPs exhibiting faster efflux and shorter intracellular residence times. Shape-dependent uptake studies further expanded this understanding. Spherical gold NPs are taken up five times more efficiently than rod-shaped gold NPs (Figure 1B). Among rods, lower aspect ratio particles were more easily internalized, with uptake governed largely by rod width rather than length. Rod-shaped NPs were exocytosed more quickly than spherical ones, likely because their different contact geometry affects how cells processed them. This was confirmed by ICP-AES (Inductively Coupled Plasma-Atomic Emission Spectroscopy) measurements and transmission electron microscopy (TEM) showing fewer rods enclosed in membrane structures and a higher rate of rod efflux.

Beyond metallic systems, hydrogel nanodiscs and nanorods with equivalent volume and surface charge exhibit distinct geometry-dependent internalization across mammalian cell types. Agarwal et al showed that epithelial cells (HeLa and human embryonic kidney 293 cells), immune cells (bone marrow-derived dendritic cells), and endothelial cells (Human umbilical vein endothelial cells) consistently internalize nanodiscs more efficiently than nanorods, and that larger nanodiscs and nanorods are taken up more readily than smaller ones, in contrast to the classical size trend observed for spherical NPs (Figure 2).[47] Uptake mechanisms were shape-specific and cell-type-specific, with macropinocytosis occurring across all cell types, caveolae-mediated uptake restricted to epithelial cells, and clathrin-mediated uptake dominant in endothelial cells. Building on these static 2D observations, Jurney et al examined how shear conditions that mimic blood flow affect PEG-based hydrogel NP uptake in endothelial monolayers.[48] Using PEG nanodiscs and nanorods of matched volumes, they showed in microchannel flow that larger particles retained their uptake advantage, mirroring their static-culture behavior (Figure 3). Flow further enhanced internalization of elongated geometries because hydrodynamic rotation increased contact frequency between NP and cell. These hydrogel systems demonstrate that endothelial cells integrate geometric cues with mechanical forces, resulting in preferential uptake of larger or elongated particles under flow. Together, these findings indicate that uptake behaviours measured in static 2D cultures do not always predict NP interactions under vascular flow.

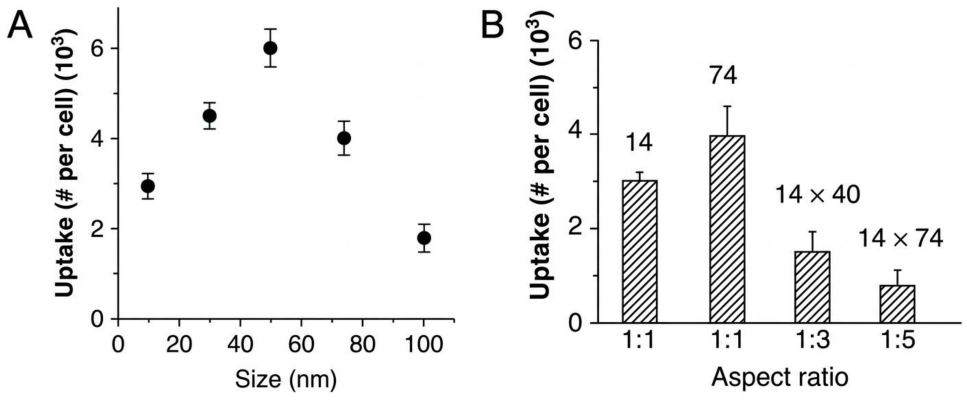

Figure 1 Size- and shape-dependent uptake of gold NPs in HeLa cells. (**A**) Quantitative cellular uptake of spherical gold NPs (14–100 nm) showing maximal internalization at ~50 nm. (**B**) Uptake of gold nanorods with differing aspect ratios, showing lower uptake than spheres and dependence on rod width. Reproduced with permission from ref.[27] Copyright 2006 American Chemical Society.

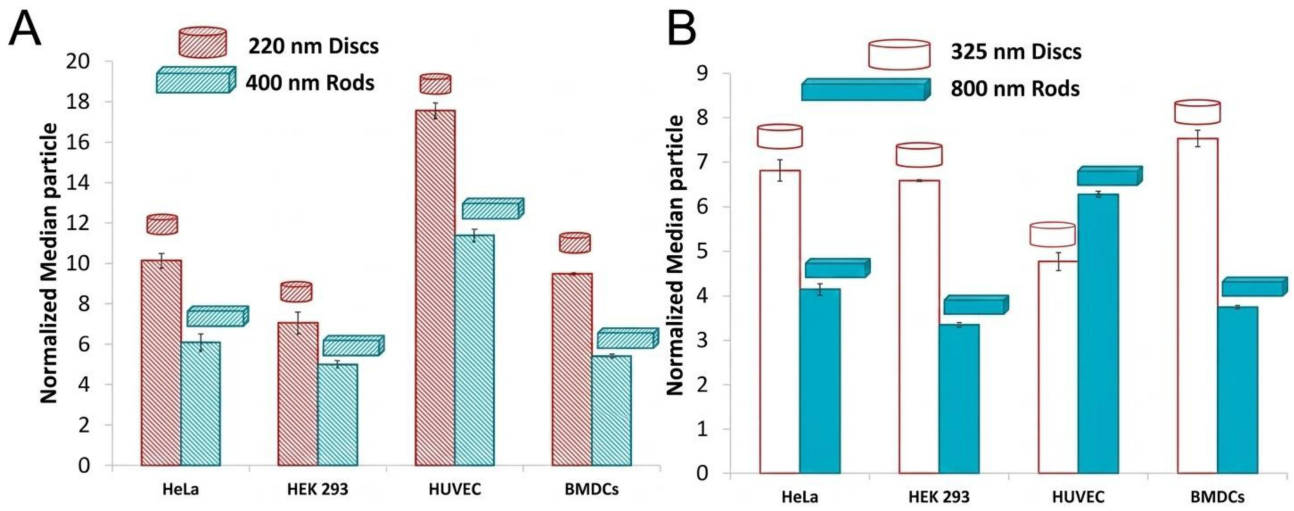

Figure 2 Shape-dependent uptake of hydrogel NPs. (**A**) Uptake of nanodiscs and nanorods in HeLa, HEK 293 (human embryonic kidney 293 cells), HUVEC (Human umbilical vein endothelial cells), and BMDC (bone marrow-derived dendritic cells), showing consistently higher internalization of discs. (**B**) Uptake trends in the same cell lines with larger disc and rod geometries, demonstrating disc-dominant uptake. Reproduced with permission from ref.[47]

NPs introduced into blood plasma rapidly adsorb proteins, forming a protein corona that redefines their biological identity.[49] Tenzer et al showed that plasma proteins begin binding within ten seconds. Using aminated (cationic) and carboxylated (anionic) polystyrene NPs, they demonstrated that initial surface charge dictates the earliest corona composition, with both cationic and anionic particles rapidly forming protein layers enriched in abundant proteins such as albumin and fibrinogen.[50] Time-resolved ultracentrifugation and mass spectrometry (MS) showed that more than 30 plasma proteins adsorb onto NP surfaces within seconds, confirming that the emerging soft corona, rather than the bare NP surface, governs the earliest NP-cell interactions. Consistent with this, uptake in RAW264.7 macrophages correlated with the adsorbed protein layer rather than with native NP charge. The dynamic soft corona, composed of loosely bound proteins that exchange with the surrounding biological fluid, strongly modulates uptake, while coronas enriched in opsonins such as C3, fibrinogen, and IgG enhanced phagocytic internalization. Protein corona effects also extended to porous polymeric NP systems. Yan et al showed that porous poly(methacrylic acid) nanoporous polymer particles form an albumin-rich corona when incubated in cell growth media containing fetal bovine serum (FBS), and that this corona alters uptake in a cell type dependent manner.[51] In the human monocytic THP 1 cell line, the albumin rich corona masked NP surface groups needed for membrane attachment, reducing adhesion and lowering uptake relative to uncoated particles. In differentiated macrophage like THP 1 cell lines (dTHP 1), the same corona engaged class A scavenger receptors and rerouted particles into receptor-mediated phagocytosis, altering the uptake pathway rather than the overall NP internalization level. These results highlight how corona composition and cell-specific receptor expression jointly shape NP interactions in 2D immune models.

Along with NP physicochemical properties, cellular physiology and therapeutic modulation also strongly influence NP internalization. Neshatian et al examined the effects of hypoxia on the uptake of 15, 50, and 74 nm gold NPs in MCF 7 (Michigan Cancer Foundation 7) and HeLa cell lines.[52] 50 nm gold NPs showed the highest uptake under both normoxic and hypoxic conditions. Reduced oxygen levels further increased intracellular retention by suppressing exocytosis and promoting vesicular trapping, indicating that hypoxic tumor microenvironments can enhance NP accumulation. In prostate cancer cell lines, low dose docetaxel induced G_2/M cell cycle arrest and increased uptake of RGD-PEG functionalized gold NPs, demonstrating that cell cycle synchronization and ligand-mediated targeting improve NP retention.[53]

Together, these studies underline that NP uptake is dictated by size, shape, and surface, along with their interdependent influence from protein corona formation, endocytic dynamics, and cellular physiology. Although 2D monolayer systems have been instrumental in defining core principles of NP uptake, they cannot capture tissue-level features such as extracellular matrix density, multicellular packing, or interstitial gradients. Insights from hydrogel systems, metallic NPs,

https://doi.org/10.2147/IJN.S558763

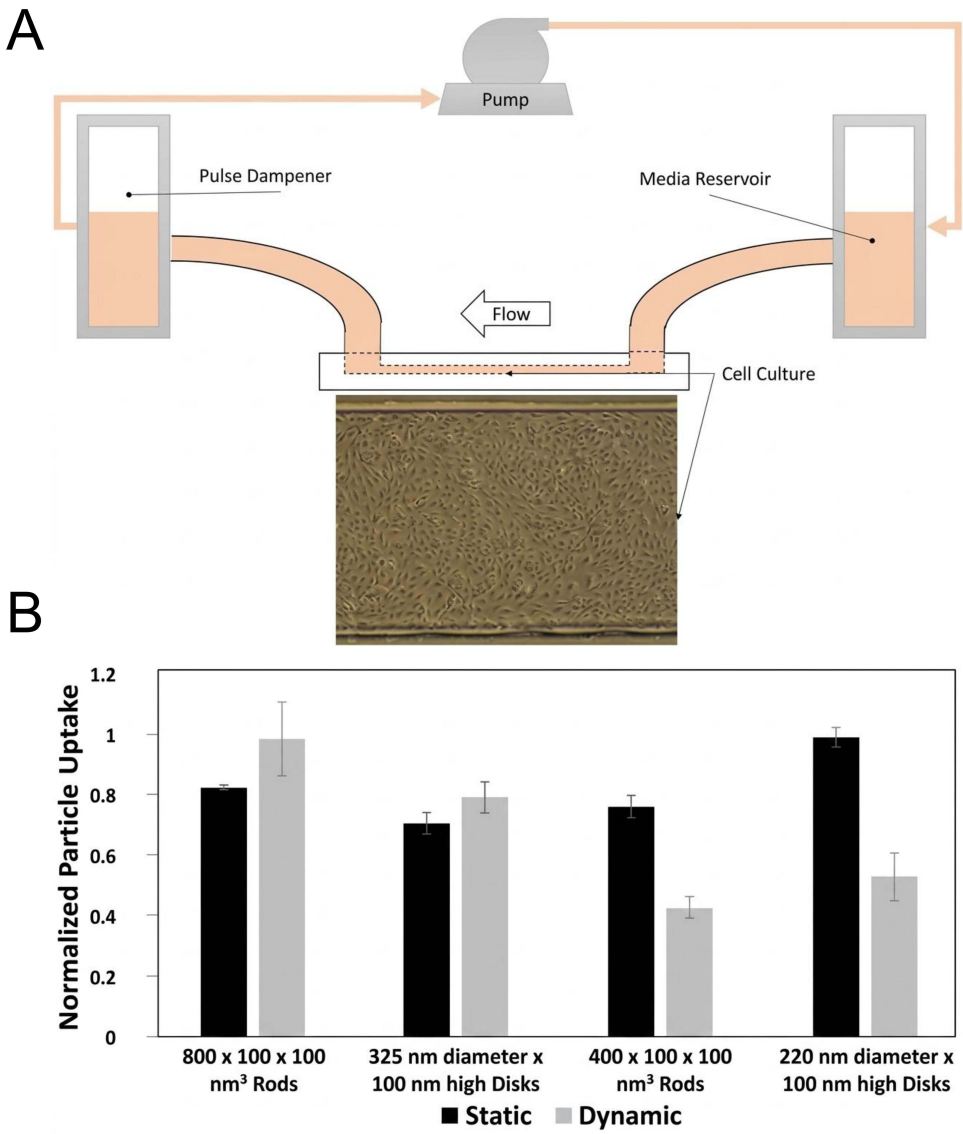

Figure 3 Flow-dependent uptake of non-spherical PEG hydrogel NPs by endothelial cells. (**A**) Schematic illustration of the microfluidic flow system used to expose HUVECs (Human umbilical vein endothelial cells) to physiological shear stress (10 dynes/cm^2). (**B**) Normalized uptake of rods and disks under static and dynamic flow, showing higher internalization of larger, high-aspect-ratio particles under shear. Reproduced with permission from ref.[48] Copyright 2017 Elsevier.

and corona-driven uptake demonstrate that static 2D conditions often overestimate internalization and overlook diffusion barriers. These mechanistic observations collectively justify transitioning to 3D spheroids and multilayer culture systems that better emulate tumor structure, spatial heterogeneity, and diffusion limitations, thereby improving the predictive value of in vitro NP transport studies. Importantly, several physicochemical parameters that enhance uptake in 2D monolayers do not necessarily improve transport in 3D systems. Features such as high surface charge or ligand density may increase cellular uptake in monolayers but promote extracellular matrix binding or peripheral trapping in spheroids. This underscores the importance of evaluating NP performance across multiple biological models.

NP Transport and Penetration in Multilayer and 3D Spheroid Models

Multilayer and 3D spheroids mimic the gradients of oxygen, nutrients, and ECM density characteristic of solid tumors, providing a more realistic platform to assess NP penetration and retention. A multilayer model using stratified breast cancer cell layers was developed to mimic tissue-like architecture (Figure 4).[54] In this system, 20 nm citrate-stabilized gold NPs diffused deeper into the multilayer construct, whereas 50 nm gold NPs, although optimal for uptake in 2D monolayers, failed

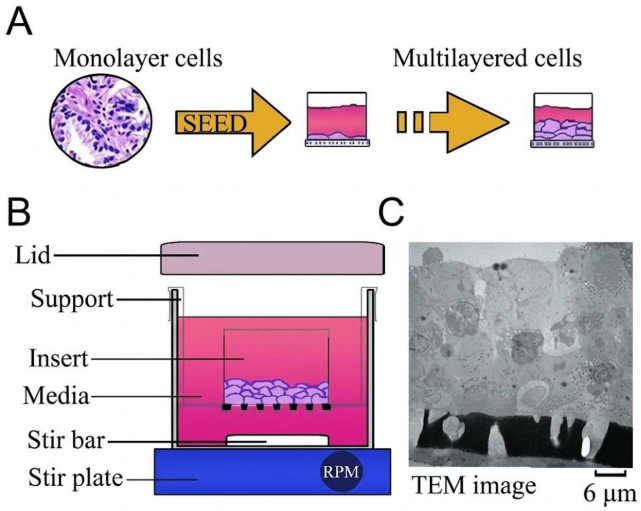

Figure 4 Multilayer cell model. (**A**) Schematic illustrating the generation of multilayered breast cancer cell constructs from an initial monolayer by sequential seeding. (**B**) Setup used to culture stratified cell layers, showing the insert, media chamber, and stirring system. (**C**) TEM image of the resulting multilayered tissue-like structure. Reproduced from ref[54] under a Creative Commons Attribution (CC-BY) license.

to penetrate to comparable depths. Similar findings were reported in multicellular pancreatic tumor layers, where PEG- and RGD-modified gold NPs showed 50–60% lower accumulation in 3D tissue compared to 2D monolayers due to increased structural complexity.[55] These observations demonstrate that size-dependent uptake trends identified in 2D assays cannot be directly extrapolated to 3D systems, where additional transport barriers limit NP distribution.

This divergence between 2D and 3D behaviour was further illustrated using polystyrene NPs in engineered spheroids, approximately 400 µm in diameter, where 100 nm and 200 nm particles remained immobilised at the spheroid periphery and penetrated only 40–50 µm, despite the known higher uptake of 100 nm particles in 2D cultures.[56] Hydrophobic interactions and ECM density contributed to this restricted transport. More advanced 3D assays have since characterised these effects with greater precision. Using a Hoechst-FACS-based assay in HCT116 (human colorectal tumor) spheroids, Tchoryk et al compared 30, 50, and 100 nm polystyrene NPs with neutral, aminated, or carboxylated surfaces.[57] They demonstrated that smaller (30–50 nm) neutral or PEGylated NP penetrated spheroid cores, whereas strongly charged 100 nm particles remained at the outer layers due to electrostatic interactions with the negatively charged ECM (Figure 5). These findings underscored that surface charge modulates not only cellular uptake but also ECM-mediated immobilisation.

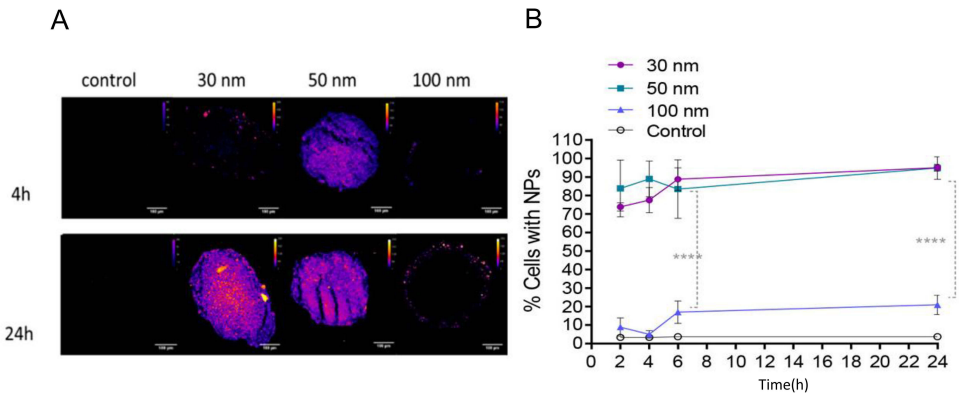

Figure 5 Size-dependent penetration of polystyrene NPs in spheroids. (**A**) Two-photon fluorescence images of spheroids incubated with 30, 50, or 100 nm NPs for 4 and 24 h, showing deeper penetration of smaller particles. (**B**) Percentage of spheroid cells containing NPs over 24 h, demonstrating higher association for 30 and 50 nm particles and minimal uptake of 100 nm particles. Data are presented as mean ± SD. Statistical significance is indicated as ****$p < 0.0001$. Reproduced from ref[57] under a Creative Commons Attribution (CC-BY) license.

https://doi.org/10.2147/IJN.S558763

Recent multidimensional analyses using gold NPs in MCF-7 spheroids reinforced this size limitation. Zhu et al used ICP-MS (Inductively Coupled Plasma-mass spectrometry), fluorescence imaging, X-ray fluorescence tomography, and TEM to evaluate transport of 2–100 nm gold NPs and found that only particles ≤ 20 nm penetrated beyond the peripheral layers, while 50–100 nm NPs accumulated primarily at the spheroid rim.[58] A similar trend was reported in A549 lung carcinoma spheroids, in which gold NPs (10–30 nm) traversed the spheroid core, while 50–65 nm particles remained confined peripherally.[59] Among surface chemistries tested, citrate-coated gold NPs exhibited the greatest balance between deep diffusion and cellular uptake, outperforming cetyltrimethylammonium bromide (CTAB) and PEG-coated variants. These results demonstrate that small size and mild negative charge favour deeper penetration in 3D tumor-like structures.

Additional insights into 3D penetration dynamics were provided by live spheroid tracking using the DONUTS (Determination of NP Uptake in Tumor Spheroids) platform, a high-content imaging system that captures real-time NP transport across intact, living spheroids without sectioning. This platform uniquely enables spatial and temporal mapping of NP movement through the spheroid volume, revealing that 10 nm silica NPs penetrated deeply into U87 glioblastoma, SK-N-BE(2) neuroblastoma, and H460 non-small cell lung cancer spheroids, whereas 30 nm and 100 nm particles remained confined to the outer layers.[60] Importantly, spheroid biophysical properties played a major role, as loosely packed neuroblastoma spheroids permitted deeper transport than densely packed glioblastoma or lung carcinoma spheroids. A separate multidimensional analysis using breast adenocarcinoma spheroids demonstrated that size also determines the dominant route of tissue entry. In this model, 15 nm gold NPs crossed cells directly through passive transcellular transport, while 60 nm NPs depended on energy-driven transcellular uptake. Intermediate 22 nm NPs used both transcellular movement through cells and paracellular movement between cells, which enabled them to reach the deepest regions of the spheroid.[61] These findings show that optimal penetration in 3D tumor models does not depend solely on smaller size but on how size governs the transport routes that NP can access.

Across three studies, Bromma et al showed that 3D spheroids reveal NP-drug interactions that differ substantially from 2D monolayers.[53,62,63] In their 2021 work using CAL-27 (human tongue squamous cell carcinoma) and HeLa (human cervical adenocarcinoma) spheroids, docetaxel pretreatment greatly enhanced the uptake and penetration of 15 nm RGD-functionalized gold NPs, increasing internalization in 3D by 47–186% compared to only 13–24% increase in monolayers (Figure 6), and improving penetration depth by 33% in CAL-27 and 17% in HeLa.[62] Their 2022 prostate cancer study further demonstrated that docetaxel at GR50 (growth rate 50) concentrations significantly increased uptake of approximately 27 nm RGD-PEG gold NPs in PC-3 (prostate adenocarcinoma) and LNCaP (lymph node carcinoma of the prostate) spheroids by 134% and 109%, respectively.[63] The effect was more pronounced in spheroids than in monolayers because the outer proliferative layers, which preferentially accumulate NPs, also receive the highest drug exposure. Their 2023 work extended these findings by combining gold NPs, docetaxel, and radiation in HeLa and LNCaP spheroids, resulting in substantially greater reductions in spheroid viability and volume than any single treatment, confirming a synergistic radiosensitization effect.[53] Collectively, these studies highlight that multicellular spheroids provide a more physiologically relevant platform for evaluating NP uptake, drug sensitization, and combined therapeutic responses compared to conventional 2D monolayers.

Overall, multilayer and 3D spheroid systems reveal several overarching trends. First, smaller NPs penetrate deeper than larger ones due to steric restrictions imposed by tightly packed cellular and ECM networks. Second, neutral or mildly negative surface charges facilitate deeper transport by minimizing electrostatic adhesion to the anionic ECM, whereas strongly cationic NPs exhibit peripheral trapping. Third, tumor biophysical properties, including cell density and stiffness, exert major control over penetration depth. Finally, the role of NP shape remains relatively underexplored in 3D tumor models, representing an important direction for future studies aiming to integrate geometry with physiologically relevant transport dynamics. This gap likely reflects technical challenges in producing anisotropic NPs with consistent size and surface chemistry, as well as difficulties in imaging and quantifying geometry-dependent transport in dense 3D tissues. It therefore remains unclear whether the penetration advantages of rods, discs, or filaments observed in 2D systems persist in more complex tumor architectures. Addressing this question is essential, as optimizing uptake and penetration are distinct design challenges that must be evaluated in parallel.

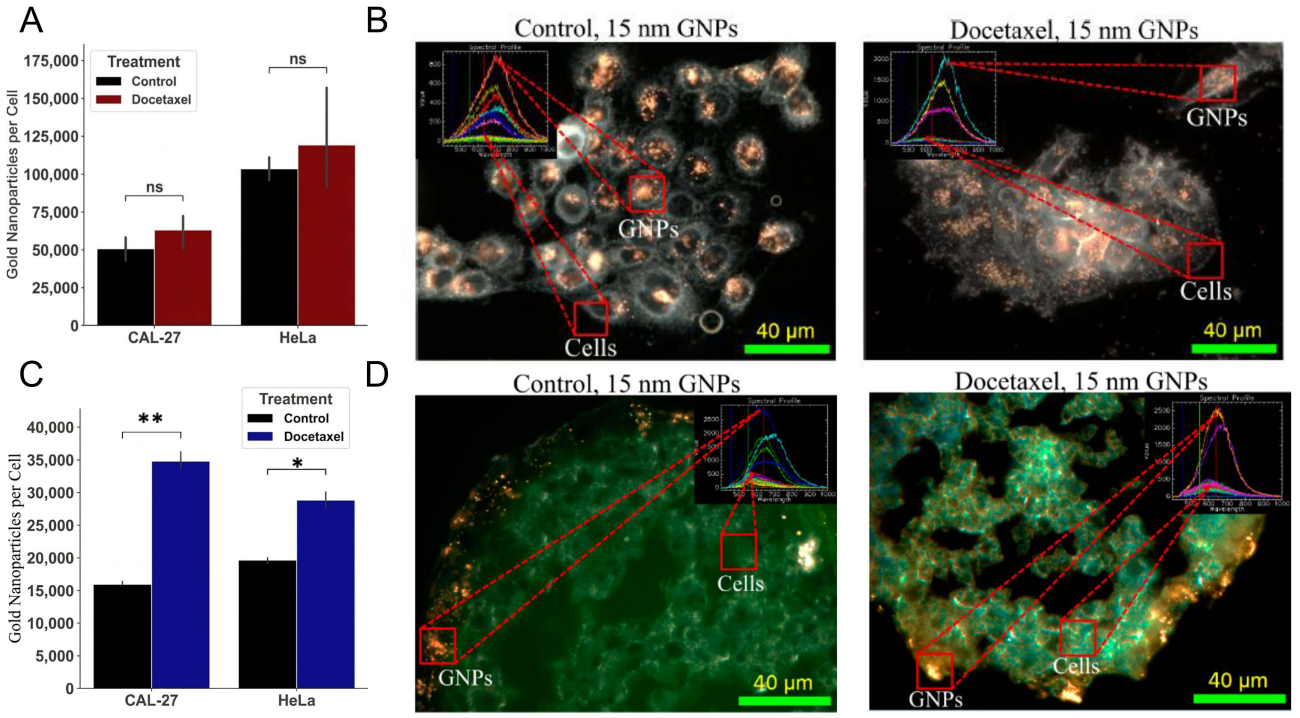

Figure 6 Docetaxel enhances uptake of 15 nm RGD-functionalized gold NPs in CAL-27 and HeLa models. (**A**) Quantification of 15 nm gold NP internalization in CAL-27 and HeLa monolayers after 24 h, showing modest and non-significant increases following docetaxel treatment. (**B**) Darkfield and hyperspectral images of CAL-27 monolayers demonstrating intracellular gold NPs with and without docetaxel pretreatment. (**C**) Quantification of 15 nm gold NP uptake in CAL-27 and HeLa spheroids, showing significantly higher internalization following docetaxel treatment. (**D**) Darkfield and hyperspectral images of HeLa spheroids confirming greater gold NP accumulation after docetaxel pretreatment. Data are presented as mean ± SD. Statistical significance is indicated as *$p < 0.05$, **$p < 0.01$; ns, non-significant. Reproduced from ref[62] under a Creative Commons Attribution (CC-BY) license.

How in vivo Models Determine NP Biodistribution and Tumor Delivery

Non-Immunocompetent Mouse Models (Xenografts)

Xenograft models in immunodeficient mice remain a widely used platform for studying NP biodistribution, tumor accumulation, and therapeutic response under controlled, immune-silent conditions. These systems reproduce key features of human tumor physiology, including abnormal vasculature, elevated interstitial pressure, and heterogeneous stromal organization, all of which influence NP transport through the enhanced permeability and retention (EPR) effect.[64] The EPR effect arises because tumor blood vessels are highly leaky and poorly organized, allowing NPs to extravasate more readily into tumor tissue, while impaired lymphatic drainage slows their clearance and promotes retention. In the absence of adaptive immunity, NP clearance is governed primarily by the reticuloendothelial system (RES),[65] enabling clearer interpretation of how different nanoformulations affect vascular extravasation, stromal penetration, and intratumoral retention. As such, xenograft models provide an essential bridge between simplified in vitro assays and the more complex pharmacological and immunological environments encountered in immunocompetent systems.

In vivo xenograft studies consistently show that NP geometry, size, and surface chemistry jointly dictate tumor delivery. A representative example is a nude mouse xenograft model of human epithelial carcinoma, where PEGylated gold nanorods measuring 24×7 nm accumulated in tumors at approximately twelve times the percent injected dose per gram of tissue (% ID/g tissue) compared with larger ~150 nm gold nanoshells, despite both exhibiting comparable liver uptake (Figure 7).[66] This enhanced tumor deposition reflects more efficient vascular extravasation and interstitial transport of smaller anisotropic particles. Repeated injections progressively increased tumor NP loading until a saturation plateau was reached while liver uptake remained stable, indicating that multi-dose administration can boost tumor delivery without increasing off-target organ accumulation. The influence of NP size and ligand presentation has also been dissected in MDA-MB-435 human melanoma xenografts. Sykes et al compared PEG-coated (passive) and transferrin-functionalized (active) gold NPs of multiple sizes and found that only the ~60 nm actively targeted

https://doi.org/10.2147/IJN.S558763

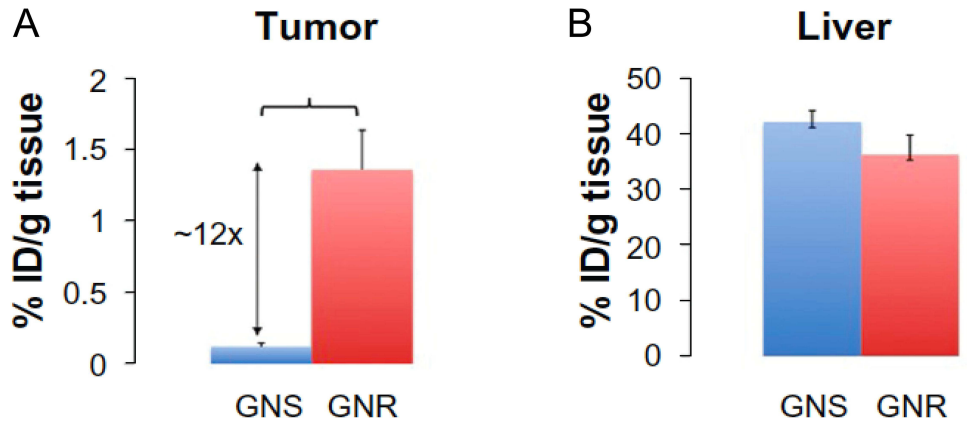

Figure 7 Tumor and liver accumulation of PEGylated gold nanoshells (GNS) and nanorods (GNR) following intravenous injection in a nude mouse xenograft model.(**A**) Percent injected dose per gram of tumor tissue (%ID/g) measured 24 h after injection, showing roughly twelve-fold higher tumor accumulation of GNR compared to GNS. (**B**) Liver accumulation of both NP types at 24 h, demonstrating comparable uptake independent of geometry. Reproduced from ref[66] under a Creative Commons Attribution (CC-BY) license.

formulation produced a measurable improvement in tumor accumulation over PEGylated controls. Smaller particles (15–30 nm) and larger particles (100 nm) showed no benefit from transferrin, indicating that receptor-mediated targeting outperforms passive EPR-driven delivery only within a narrow size range that preserves both vascular transport and receptor accessibility.[67] Complementary work with narrowly distributed PEG–PLA (polyethylene glycol–poly(lactic acid)) NPs of 111, 141, and 166 nm in A2780 (ovarian carcinoma) and HT29 (colon carcinoma) xenografts showed that ~110 nm particles exhibited the highest tumor accumulation. These particles achieved roughly 1.6 to 2.5-fold greater uptake than 141 and 166 nm NPs in A2780 tumors and about 1.2 to 1.5-fold higher uptake in HT29 tumors. Larger particles preferentially redistributed to liver and spleen, consistent with enhanced clearance by the RES.[68] Studies in HepG2 xenografts further illustrate how rod geometry and surface chemistry shape in vivo behavior. Among gold nanorods of similar aspect ratio but different lengths (about 60, 70, and 97 nm), medium-sized rods (~70 nm × 11.5 nm) showed the greatest tumor accumulation and longest retention, and lactoferrin coated rods reached up to ~9.4% ID/g tissue and enabled complete photothermal ablation under second near-infrared (NIR-II) irradiation, whereas both smaller and larger rods displayed lower accumulation and incomplete regression.[69] Collectively, these findings demonstrate that successful in vivo tumor targeting arises from coordinated control of NP physical attributes and surface functionalization, each shaping transport, retention, and therapeutic response. Beyond tumor selective delivery, systemic biodistribution patterns impose fundamental constraints that shape how NPs behave in vivo.

A foundational body of work has also established how particle size governs whole-body biodistribution beyond tumors. De Jong et al showed that 10 nm gold NPs distribute widely across liver, spleen, kidney, lung, brain, and heart after intravenous injection, while larger particles (50 to 250 nm) accumulate almost exclusively in liver and spleen due to rapid RES sequestration.[70] This study provided the first quantitative evidence that sub-20 nm NPs can access multiple organs that are inaccessible to larger formulations, emphasizing the need to consider systemic exposure and clearance risks when designing tumor-directed nanomedicines. Complementing these findings, Choi et al demonstrated that NPs with hydrodynamic diameters below ~55 nm undergo efficient renal clearance, establishing the classical renal cut-off. Although shown using quantum dots, this principle applies broadly across nanomaterials.[71] Longmire et al further showed that clearance reflects the combined effects of particle size, surface charge, and protein corona formation, which together determine whether NPs undergo renal elimination or hepatosplenic retention.[72] Collectively, these studies define the systemic constraints that shape NP behavior in vivo and provide essential context for interpreting tumor-specific biodistribution in xenografts.

Pharmacological modulation of tumor biology can further enhance NP delivery in vivo. In PC-3 prostate cancer xenografts, pretreatment with docetaxel (6 mg kg^{-1}, intravenous) markedly increased the accumulation of RGD-PEG-functionalized gold NPs (1.5 mg kg^{-1}), nearly doubling intratumoral gold levels by synchronizing cells in the G_2/M phase and thereby improving retention while reducing efflux.[53,63] The route of administration can also override ligand

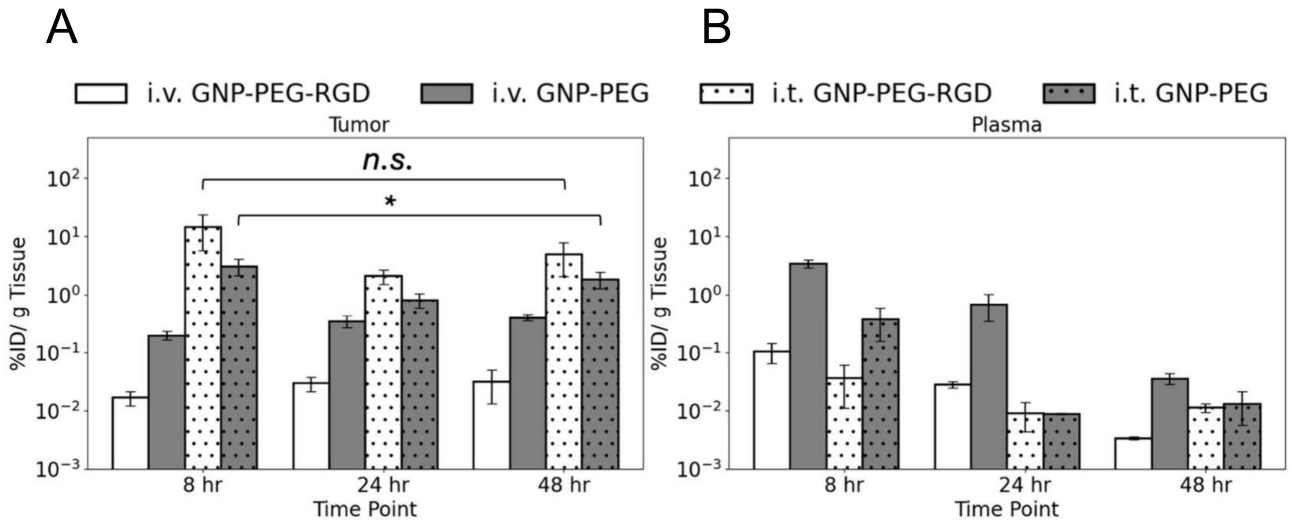

Figure 8 Tumor and plasma levels of PEGylated and RGD-functionalized gold NPs after intravenous (i.v.) and intratumoral (i.t.) administration. (**A**) Tumor accumulation of PEG-gold NP (GNP) and PEG-GNP following i.v. and i.t. injections. RGD-PEG NPs show markedly reduced tumor levels after i.v. injection due to rapid systemic clearance, whereas PEG NPs accumulate more efficiently. i.t. delivery increases tumor uptake for both formulations, with a significant improvement for PEG NPs because they already exhibit higher retention following i.v. dosing. (**B**) Plasma concentrations following i.v. and i.t. injections. RGD-PEG NPs exhibit lower circulating levels than PEG NPs after i.v. delivery, reflecting faster clearance. i.t. administration minimizes systemic exposure for both NP types. Data is reproduced with permission. Data are presented as mean ± SD. Statistical significance is indicated as *$p < 0.05$; ns, non-significant. Reproduced with permission from ref[73] Copyright 2025 American Chemical Society.

design. In immunodeficient mice with endometrial carcinoma xenografts, intravenous injection of RGD-functionalized gold NPs led to a 91% reduction in tumor accumulation due to rapid mononuclear phagocyte system clearance, whereas intratumoral administration achieved far higher tumor retention and substantially reduced systemic uptake (Figure 8).[73] Together, these findings demonstrate that both pharmacological cell-cycle control and the route of administration significantly influence how NPs distribute and persist within tumors and can determine whether surface functionalization produces its intended targeting benefit.

Extending these principles to biomolecular nanostructures, RNA NPs with uniform chemistry have been used to isolate the specific contributions of size and shape to in vivo biodistribution.[74] Using subcutaneous KB xenografts in immunodeficient nude mice, RNA polygons were engineered as 5, 10, and 20 nm nanosquares, along with 10 nm triangles, squares, and pentagons, enabling independent control by varying size without altering shape, and varying shape without changing overall size. Despite having identical surface composition, these RNA NPs exhibited clear size-dependent biodistribution patterns. Larger 20 nm structures circulated longer, showed delayed renal clearance, and produced stronger whole-body signals, whereas 5 nm constructs cleared rapidly through the kidneys but still reached tumors. Shape exerted more modest effects, with triangular particles clearing fastest and pentagons displaying slightly higher splenic retention. Overall, this study demonstrates that RNA-based NPs follow similar fundamental size and geometry rules that dictate biodistribution in traditional nanomaterials, reinforcing the generality of these design principles across material classes.

Xenograft studies consistently show that NP behavior in vivo emerges from the interplay between physicochemical design and the biological environment. NP size strongly influences circulation time, organ-level distribution, and the extent to which particles reach tumors, while geometry and surface ligands modulate vascular passage, stromal transport, and intratumoral retention.[75,76] Tumor physiology further shapes NP fate, as features such as vascular permeability, interstitial architecture, and cell cycle status alter both accumulation and clearance dynamics.[77,78] Delivery route adds an additional layer of control, with intratumoral administration, systemic injection, and repeated dosing each producing distinct biodistribution profiles.[79] Classic biodistribution studies also reinforce that NP transport cannot be viewed solely through a tumor-centered lens; systemic clearance pathways, renal filtration limits, protein corona formation, and RES uptake patterns determine the background against which tumor targeting occurs.[70–72] These insights underscore why xenograft models are mechanistically informative yet incomplete, and why transitioning to immunocompetent systems is essential for capturing the immune-mediated transport

https://doi.org/10.2147/IJN.S558763

and clearance processes that ultimately dictate NP performance in clinical settings. However, clinical evidence indicates that the EPR effect is far less consistent in human tumors than in xenografts, owing to heterogeneous vascularity, poor perfusion, high interstitial pressure, and dense stroma that restrict NP entry and movement.[77,80] A meta-analysis by Wilhelm et al found that the median NP delivery to solid tumors across hundreds of studies was below one percent of the injected dose, highlighting the impact of these barriers.[81] These findings indicate that xenografts often overestimate delivery efficiency and emphasize the need for complementary evaluation in immune-intact systems.

Immunocompetent Mouse Models and Immune Barriers

NPs rapidly interact with plasma proteins and blood components upon systemic administration, forming dynamic coronas that can trigger complement activation, immune recognition, and macrophage uptake.[82] In vivo, this corona continues to evolve as NPs circulate, undergoing protein exchange and opsonin enrichment that differ substantially from in vitro profiles. These changes can mask targeting ligands, alter NP charge and hydrodynamic size, and redirect particles toward rapid clearance, linking corona remodeling directly to immune engagement.[49,83] Chronic inflammatory signaling and immune-tumor crosstalk further reshape NP interactions within the tumor microenvironment, influencing biodistribution, clearance kinetics, and therapeutic response. These early host-particle interactions strongly influence NP biodistribution and frequently accelerate clearance through the mononuclear phagocyte system (MPS), often overriding the intended effects of ligand-mediated targeting. These immune-driven surface effects are not restricted to metallic NPs but are also evident in clinically advanced lipid NPs and polymeric formulations. Studies on lipid NPs and PEGylated systems show that surface architecture, PEG density, and lipid composition influence complement activation, protein adsorption, and corona remodeling, and innate immune recognition, which together shape circulation time and organ sequestration.[2,23,38,84] Even in clinically optimized formulations, these dynamic surface transformations and immune responses can limit effective tumor delivery, underscoring that immune compatibility remains a key design constraint across NP platforms.

Immunocompetent tumor models, therefore, provide a more robust platform than immunodeficient xenografts because the full innate and adaptive immune machinery remains intact. This enables assessment of complement-driven opsonization, phagocytic sequestration, cytokine-mediated transport barriers, and NP-immune cell crosstalk within the tumor microenvironment. They also capture immune-driven changes in vascular permeability, redistribution of NPs by tumor-associated macrophages (TAMs), and inflammation-dependent clearance patterns, providing a clinically relevant readout of NP delivery, clearance, and therapeutic response.

Talamini et al used an immunocompetent mouse model with endotoxin-free gold NPs to understand how size and shape influence biodistribution under normal physiological conditions without tumor-associated permeability or inflammation.[85] Four NP types were tested, including 10 nm spheres, 50 nm spheres, 60×30 nm rods, and star-shaped NPs of about 55 nm, all with identical surface chemistry. Time-resolved ICP-MS measurements at 1, 24, and 120 h showed clear geometry-dependent trends. The 10 nm spheres circulated the longest, with gradual accumulation in liver and spleen that increased steadily from 24 to 120 h. The 50 nm spheres were rapidly retained in liver and spleen within the first hour and stayed at high levels thereafter. Rod-shaped NP exhibited minimal organ penetration at 1 h and were almost entirely cleared by 24 h, indicating rapid elimination. Star-shaped NP showed a distinct profile with early lung accumulation already evident at 1 h and further rising by 120 h, along with uptake in liver and spleen. These differences demonstrate that NP geometry modulates interactions with endothelial barriers and macrophage-rich tissues, which in turn shapes circulation time and determines how much of the NP pool remains available for tumor delivery. A complementary biodistribution study in immunocompetent mice bearing B16 melanoma allografts was reported by Poon et al.[86] This work examined how surface chemistry modulates in vivo fate by comparing ultrasmall 2.7 nm gold NP that were either unmodified, PEGylated, or conjugated to myxoma-derived or cRGD peptides. Biodistribution at 4, 24, and 72 h showed that PEG increased early blood persistence and slowed renal elimination, consistent with its classical role in extending circulation time. Peptide coatings produced distinct behaviors, with cRGD displaying early tumor entry followed by rapid clearance, while the myxoma peptide supported higher tumor retention from 24 to 72 h. Across all formulations, liver, spleen, and kidney remained the major clearance organs, in agreement with size-dependent biodistribution trends observed in non-tumor bearing models.[70] Tumor-associated mass fractions were low overall, typically

0.75–2% of the injected dose, with myxoma and PEG-cRGD formulations showing the highest transient accumulation. Braun et al provided an additional example using enzyme-responsive targeting. They designed a peptide that becomes active only after cleavage by urokinase, a protease that is strongly upregulated in many solid tumors including 4T1 breast cancer.[87] Cleavage exposes a short CendR sequence, a natural binding motif that binds neuropilin-1, a receptor expressed on tumor blood vessels. Once exposed, this CendR motif triggers neuropilin-1-mediated internalization. In 4T1 tumors, fluorescent NP coated with this urokinase-responsive peptide accumulated selectively in tumors only after enzymatic activation, whereas the inactive form showed minimal uptake. This demonstrates that incorporating protease-responsive elements can introduce an additional layer of tumor selectivity.

More recently, two complementary studies by Jackson et al provided quantitative evidence for how immune status alters NP distribution in vivo. The authors compared NP biodistribution in immunocompetent KPCY (mouse model of pancreatic adenocarcinoma) tumor-bearing mice versus immunodeficient MIA PaCa-2 (human pancreatic adenocarcinoma) xenografts (Figure 9A and B).[88] An intact immune system reduced tumor accumulation by up to 95% due to rapid sequestration of gold NP by liver and spleen macrophages, underscoring the dominant role of MPS clearance in immunocompetent animals. Co-administration of docetaxel improved NP persistence, increasing intratumoral in vitro retention in 2D cultures by about 180% and raising in vivo tumor levels by nearly 70% without altering whole-body distribution (Figure 9C and D). They extended these findings by examining how RGD-functionalized NP behave under

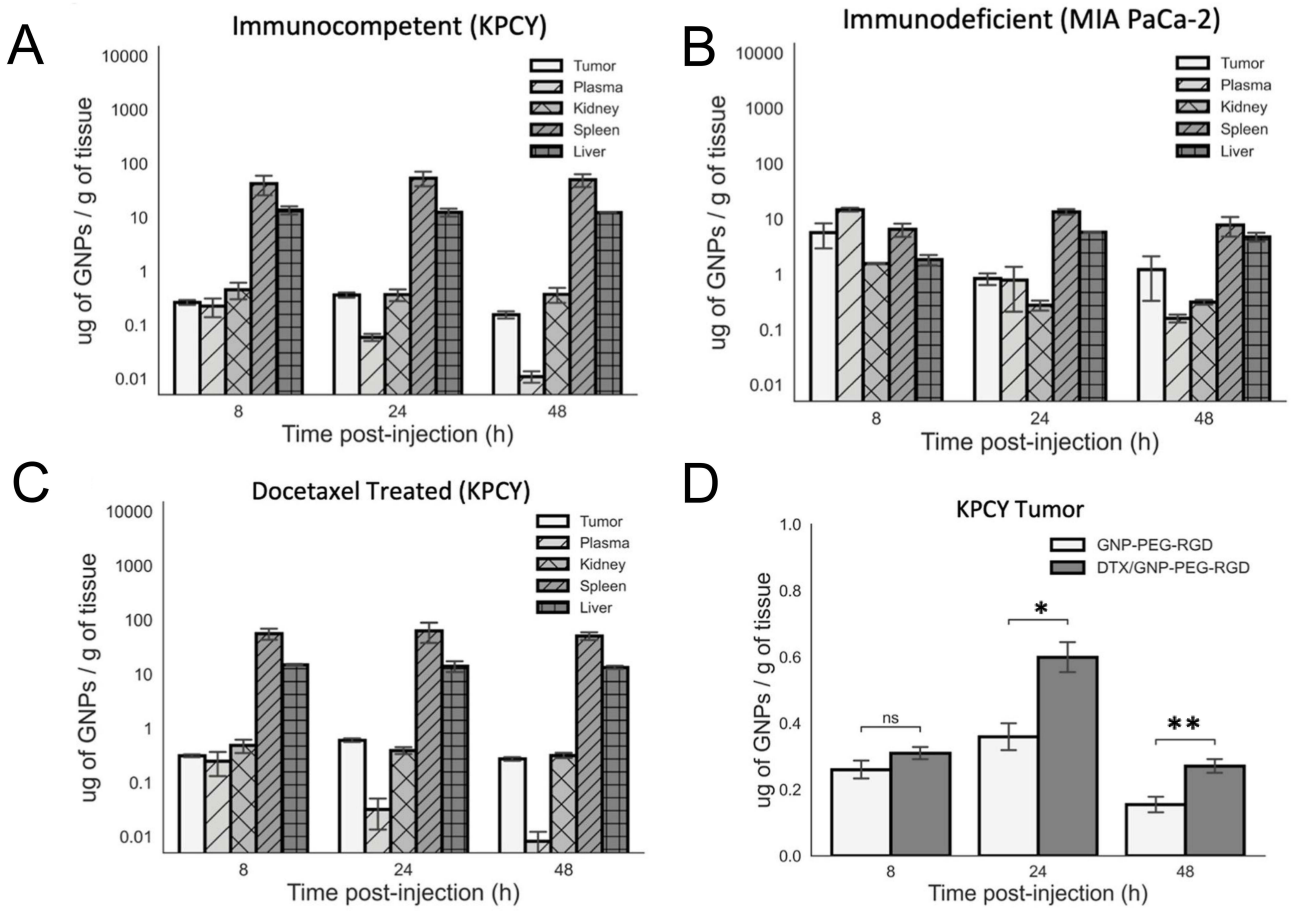

Figure 9 Biodistribution of gold NP in immunocompetent and immunodeficient hosts and the effect of docetaxel on tumor retention. (**A**) In immunocompetent KPCY tumor-bearing mice, most injected NPs were sequestered by liver and spleen within 8–48 h, with low NPs retention in tumors, highlighting dominant MPS clearance. (**B**) Immunodeficient MIA PaCa-2 xenografts showed higher tumor accumulation and reduced hepatic and splenic uptake compared to immunocompetent mice, demonstrating the impact of an intact immune system on NP biodistribution. (**C**) Docetaxel pretreatment in immunocompetent KPCY mice increased NP levels in tumors at 24–48 h while not substantially altering whole-body distribution, indicating reduced NP efflux rather than changes in systemic clearance. (**D**) Direct tumor measurements confirmed that docetaxel enhanced intratumoral NP retention at 24 and 48 h relative to untreated controls, supporting the role of cytoskeletal inhibition in limiting NP exocytosis. Data are presented as mean ± SD. Statistical significance is indicated as *$p < 0.05$, **$p < 0.01$; ns, non-significant. Reproduced with permission from ref.[88] Copyright 2025 American Chemical Society.

https://doi.org/10.2147/IJN.S558763

the same conditions.[89] Although RGD increased uptake in vitro by 20–40-fold over 24 h, the particles showed almost no improvement in vivo, with tumor accumulation remaining close to background levels due to rapid MPS filtering. Detailed ICP-MS biodistribution data showed that liver and spleen absorbed the majority of injected NP within the first 8–24 h, while only a very small fraction reached the tumor, far lower than what the strong in vitro uptake would have predicted. Together, these studies show that immune clearance often overrides ligand-mediated targeting in vivo, while docetaxel can partially mitigate this by slowing NP efflux, in vivo tumor accumulation still remains far lower than in vitro uptake.

Further studies in immune-intact mice demonstrate that NP biodistribution could be governed primarily by surface chemistry rather than particle size.[90] In this study, PEG-, chitosan-, and PVA-coated NPs all shared the same poly(lactic-co-glycolic acid) (PLGA) core and comparable sizes, ensuring that differences in biodistribution could be attributed directly to surface properties. PEGylated NP showed the most favorable pharmacokinetics, with extended circulation, reduced liver and spleen uptake, and lower protein adsorption, consistent with diminished recognition by the mononuclear phagocyte system. In contrast, chitosan- and PVA-coated NP accumulated rapidly in clearance organs due to their higher surface charge and stronger interactions with plasma proteins. Uptake in macrophage-rich tissues was greatest for positively charged formulations, underscoring charge-dependent phagocytic recognition. These findings show that surface functionalization strongly influences biodistribution in immune-intact systems.

A comprehensive in vivo evaluation in immunocompetent CD-1 mice showed that silica NPs display distinct biodistribution profiles governed primarily by porosity and surface charge.[91,92] Mesoporous SiO_2 NPs displayed strong but transient lung sequestration within the first hour, driven by their large internal surface area and increased protein adsorption, which promoted early trapping in pulmonary capillaries. Nonporous Stöber particles, by contrast, showed minimal lung association and instead accumulated predominantly in the liver and spleen due to efficient RES filtration and faster redistribution from circulation. Surface amination consistently reduced lung retention and enhanced liver and spleen uptake, reflecting increased recognition by phagocytic cells for positively charged NP. Geometry exerted a secondary influence, becoming significant only in combination with surface charge, as amine-modified high-aspect-ratio mesoporous rods showed enhanced lung sequestration relative to amine-modified spheres. Pharmacokinetic and tissue-to-blood analyses further demonstrated that all formulations were rapidly cleared from circulation and that organ accumulation correlated with macrophage-rich compartments. In addition to immune-driven and physicochemical determinants, NP properties continue to change in vivo due to ongoing interactions with biological fluids. Processes such as aggregation, partial dissolution, ligand desorption, and progressive protein corona exchange alter hydrodynamic size, surface charge, and colloidal stability during circulation.[84,93,94] Detailed in vivo studies confirm that the protein corona formed in the bloodstream is compositionally distinct from that formed in vitro, producing a biological identity that can redirect NP uptake, alter pharmacokinetics, and change organ-level distribution.[95] Beyond corona remodeling, certain inorganic and polymeric NP undergo biotransformation, including structural degradation and surface reconstruction, which further modifies their interaction with phagocytic cells, renal filtration pathways, and hepatobiliary clearance.[96] These dynamic transformations significantly alter NP behavior in vivo and must be considered when evaluating NP performance in immune-intact systems.

Together, these studies demonstrate that immune-intact models are essential for clarifying how host immunity collectively governs NP distribution and processing in vivo. These systems reveal that opsonization, complement activation, macrophage engagement, renal filtration, and endothelial capture operate simultaneously and often competitively, determining how much NP ultimately reaches the tumor. These models show that small or stealth-coated NP may circulate longer but still undergo rapid hepatic filtration once opsonized, that high-aspect-ratio or mesoporous structures can become transiently trapped in microvasculature, and that charged or peptide-functionalized NP experience strong MPS engagement regardless of their in vitro targeting performance. Critically, these outcomes expose the disparity between cellular uptake studies and whole-animal behavior, underscoring that even promising ligands or responsive coatings cannot overcome systemic immune barriers without additional strategies to modulate clearance or retention. Immunocompetent models therefore provide a clinically meaningful readout of how NP formulations navigate opsonization, phagocytosis, vascular transport, and tumor entry, enabling rational design of nanomedicines that remain functional within the constraints of the intact immune system. In addition to immune-driven clearance, tumor intrinsic barriers in immunocompetent hosts further limit NP delivery. Dense extracellular matrix components such as collagen, hyaluronan,

and fibronectin restrict interstitial transport and often confine NPs to the tumor periphery, consistent with classic studies of tumor biophysical barriers.[97] Elevated interstitial fluid pressure further impedes convective flow, reducing penetration even for particles that successfully extravasate. TAMs represent another major barrier because they actively internalize NPs that enter the tumor interstitium. Miller et al demonstrated that TAMs can sequester a substantial fraction of delivered NPs, thereby lowering the amount available to malignant cells.[98] These combined ECM and macrophage-mediated barriers explain why NP accumulation rarely correlates with therapeutic efficacy in immunocompetent models and highlight the need to interpret in vivo delivery within the context of both immune surveillance and tumor microenvironment architecture.

Interpretation of NP performance in animal models must also account for species-specific differences that influence delivery and clearance. Mice exhibit faster metabolic rates, more permeable tumor vasculature, and immune compartment distributions that differ substantially from humans, which can exaggerate apparent NP delivery efficiency.[99] Moreover, structural and functional differences between murine and human tumor vasculature and microenvironment challenge the relevance of EPR-based delivery assumptions.[100,101] These interspecies variations, combined with differences in stroma, immune cell composition, and vascular heterogeneity, contribute to the observed discrepancies between promising preclinical nanomedicine results and modest clinical translation.[102] Recognizing these limitations is essential for evaluating NP fate and supports the need for more predictive, human-relevant models in nanomedicine development.

The Future Prospective

The studies summarized in this review show that NP behavior is governed by interconnected processes spanning molecular interactions, cellular uptake, tissue-level transport, and whole-body clearance. Work in 2D and 3D culture systems demonstrates how size, shape, surface chemistry, ligand presentation, and protein corona dynamics regulate internalization and intracellular fate. Although these models reveal important mechanistic trends, they cannot fully capture the complexity of in vivo transport. Xenograft studies extend these insights by incorporating vascular permeability and stromal architecture, yet their exaggerated EPR effect and immune-silent background often lead to overestimation of tumor delivery, in contrast to the low (<1%) tumor accumulation observed across preclinical and clinical datasets. Findings from immunocompetent tumor models reveal that complement activation, opsonization, and MPS-mediated sequestration frequently dominate over ligand-based targeting, rather than the favorable receptor-mediated uptake typically observed in vitro. Dense extracellular matrices, elevated interstitial pressure, and TAM-mediated uptake further restrict NP penetration, and protein corona evolution in vivo can mask targeting ligands and redirect NP toward clearance pathways. Species-specific physiological differences, including vascular permeability, immune composition, and macrophage distribution, further limit the translational relevance of murine studies. Together, these insights emphasize that NP delivery must be understood within the broader context of immune surveillance, vascular biology, and microenvironmental heterogeneity. Importantly, immune-mediated clearance emerges as a dominant translational barrier, often overriding ligand-based targeting strategies. These mechanistic insights should guide rational NP design and help explain the historically modest clinical translation of many tumor-targeted nanoformulations despite promising in vitro performance. Effective formulations must balance tumor penetration with renal and hepatosplenic clearance. Strategies that preserve NP surface integrity and targeting functionality in immune-competent environments are therefore essential, prioritizing immune compatibility and circulation stability rather than maximizing cellular uptake alone.

Recurrent translational mismatches are frequently observed when NP performance is compared across experimental model systems. For example, ligand functionalization often produces strong receptor-mediated uptake in 2D cultures, yet the same systems show minimal tumor accumulation in vivo, partly due to protein corona formation that masks targeting ligands and promotes immune recognition. Similarly, positively charged NPs that enhance cellular uptake in vitro are often rapidly cleared in vivo through opsonization and macrophage uptake by the mononuclear phagocyte system. NP size effects further illustrate this discrepancy, as particles optimized for efficient cellular internalization may still exhibit limited penetration in solid tumors. These examples highlight that design parameters maximizing cellular uptake do not necessarily optimize systemic delivery, emphasizing the need to evaluate NP performance across progressively more physiologically relevant models. Reported NP uptake and biodistribution may also vary depending on methodological factors such as quantification approaches (eg, ICP-MS versus imaging), dosing regimens and administration routes,

tumor implantation sites or models (subcutaneous versus orthotopic), and the lack of standardized reporting methods for NP accumulation and biodistribution (eg, % ID/g tissue or imaging-based signal) across studies.

Future progress will depend on advancing NP designs that remain effective within immune-intact hosts, where rapid MPS uptake, dynamic protein adsorption, and organ-specific filtration strongly influence biodistribution. Renal and hepatobiliary clearance constraints must guide decisions about NP size and surface chemistry to balance circulation time with efficient clearance and long-term safety. Consideration of NP degradation, biotransformation, and long-term fate is increasingly important because many inorganic and polymeric systems undergo structural or chemical changes in vivo that alter pharmacokinetics and organ retention. More predictive in vivo models, including orthotopic, syngeneic, and humanized tumors, are needed to better replicate vascular heterogeneity and immune interactions and to address translational gaps between murine and human tumors. Model selection can be guided by a staged framework, where 2D systems define uptake mechanisms, 3D spheroids evaluate penetration and retention, and immunocompetent models serve as the decisive platform for translational validation. Emerging tools for quantitative in vivo imaging, whole-body pharmacokinetics, and cellular-level biodistribution will help bridge discrepancies between in vitro promise and in vivo performance. Integrating material design with an understanding of systemic clearance, immune regulation, and tumor-specific barriers offers the most promising path toward nanomedicines capable of achieving selective, sustained, and clinically meaningful delivery.

Funding

This work was supported by the Natural Sciences and Engineering Research Council of Canada (NSERC) Discovery Grant (RGPIN-2017-04501) and the Canadian Institutes of Health Research (CIHR) Project Grant (PJT-399878). Additional support was provided by the University of Victoria. R.G. acknowledges support through the Aspiration Postdoctoral Fellowship at the University of Victoria.

Disclosure

The authors report no conflicts of interest in this work.

References

1. Fan D, Cao Y, Cao M, Wang Y, Cao Y, Gong T. Nanomedicine in cancer therapy. *Signal Transduct Target Ther*. 2023;8(1):293. doi:10.1038/s41392-023-01536-y
2. Mitchell MJ, Billingsley MM, Haley RM, Wechsler ME, Peppas NA, Langer R. Engineering precision nanoparticles for drug delivery. *Nat Rev Drug Discov*. 2021;20(2):101–124. doi:10.1038/s41573-020-0090-8
3. Yao Y, Zhou Y, Liu L, et al. Nanoparticle-based drug delivery in cancer therapy and its role in overcoming drug resistance. *Front Mol Biosci*. 2020;7:193. doi:10.3389/fmolb.2020.00193
4. Patra JK, Das G, Fraceto LF, et al. Nano based drug delivery systems: recent developments and future prospects. *J Nanobiotechnology*. 2018;16(1):71. doi:10.1186/s12951-018-0392-8
5. Ajith S, Almomani F, Elhissi A, Husseini GA. Nanoparticle-based materials in anticancer drug delivery: current and future prospects. *Heliyon*. 2023;9(11):e21227. doi:10.1016/j.heliyon.2023.e21227
6. Deivayanai VC, Thamarai P, Karishma S, et al. Advances in nanoparticle-mediated cancer therapeutics: current research and future perspectives. *Cancer Pathog Ther*. 2025;3(4):293–308. doi:10.1016/j.cpt.2024.11.002
7. Wang B, Hu S, Teng Y, et al. Current advance of nanotechnology in diagnosis and treatment for malignant tumors. *Signal Transduct Target Ther*. 2024;9(1):200. doi:10.1038/s41392-024-01889-y
8. Karami Fath M, Babakhaniyan K, Zokaei M, et al. Anti-cancer peptide-based therapeutic strategies in solid tumors. *Cell Mol Biol Lett*. 2022;27(1):33. doi:10.1186/s11658-022-00332-w
9. Barenholz YC. Doxil® — the first FDA-approved nano-drug: lessons learned. *J Control Release*. 2012;160(2):117–134. doi:10.1016/j.jconrel.2012.03.020
10. Gaitanis A, Staal S. Liposomal doxorubicin and nab-paclitaxel: nanoparticle cancer chemotherapy in current clinical use. In Grobmyer SR, Moudgil BM editors, *Cancer Nanotechnology. Methods in Molecular Biology*. Vol. 624. Humana Press; 2010:385–392. doi:10.1007/978-1-60761-609-2_26
11. Miele E, Spinelli GP, Miele E, Tomao F, Tomao S. Albumin-bound formulation of paclitaxel (Abraxane ABI-007) in the treatment of breast cancer. *Int J Nanomed*. 2009;4:99–105. doi:10.2147/ijn.s3061
12. Chehelgerdi M, Chehelgerdi M, Allela OQB, et al. Progressing nanotechnology to improve targeted cancer treatment: overcoming hurdles in its clinical implementation. *Mol Cancer*. 2023;22(1):169. doi:10.1186/s12943-023-01865-0
13. Menge J, Yang C, Weitz DA, Jahnke K. Engineering the biophysical properties of lipid nanostructures for drug delivery. *Commun Mater*. 2026;7(1):25. doi:10.1038/s43246-026-01073-5

14. Đorđević S, Gonzalez MM, Conejos-Sánchez I, et al. Current hurdles to the translation of nanomedicines from bench to the clinic. *Drug Deliv Transl Res*. 2022;12(3):500–525. doi:10.1007/s13346-021-01024-2
15. Thomas V, Namdeo M, Murali Mohan Y, Bajpai SK, Bajpai M. Review on polymer, hydrogel and microgel metal nanocomposites: a facile nanotechnological approach. *J Macromol Sci Part A*. 2007;45(1):107–119. doi:10.1080/10601320701683470
16. Baig N, Kammakakam I, Falath W. Nanomaterials: a review of synthesis methods, properties, recent progress, and challenges. *Mater Adv*. 2021;2(6):1821–1871. doi:10.1039/D0MA00807A
17. Williford JM, Santos JL, Shyam R, Mao HQ. Shape control in engineering of polymeric nanoparticles for therapeutic delivery. *Biomater Sci*. 2015;3(7):894–907. doi:10.1039/C5BM00006H
18. Ortiz-Castillo JE, Gallo-Villanueva RC, Madou MJ, Perez-Gonzalez VH. Anisotropic gold nanoparticles: a survey of recent synthetic methodologies. *Coord Chem Rev*. 2020;425:213489. doi:10.1016/j.ccr.2020.213489
19. Rommasi F, Esfandiari N. Liposomal nanomedicine: applications for drug delivery in cancer therapy. *Nanoscale Res Lett*. 2021;16(1):95. doi:10.1186/s11671-021-03553-8
20. Akbarzadeh A, Rezaei-Sadabady R, Davaran S, et al. Liposome: classification, preparation, and applications. *Nanoscale Res Lett*. 2013;8 (1):102. doi:10.1186/1556-276X-8-102
21. Thanh NTK, Maclean N, Mahiddine S. Mechanisms of nucleation and growth of nanoparticles in solution. *Chem Rev*. 2014;114(15):7610–7630. doi:10.1021/cr400544s
22. Zhang W, Taheri-Ledari R, Ganjali F, et al. Effects of morphology and size of nanoscale drug carriers on cellular uptake and internalization process: a review. *RSC Adv*. 2023;13(1):80–114. doi:10.1039/D2RA06888E
23. Suk JS, Xu Q, Kim N, Hanes J, Ensign LM. PEGylation as a strategy for improving nanoparticle-based drug and gene delivery. *Adv Drug Deliv Rev*. 2016;99:28–51. doi:10.1016/j.addr.2015.09.012
24. Shi L, Zhang J, Zhao M, et al. Effects of polyethylene glycol on the surface of nanoparticles for targeted drug delivery. *Nanoscale*. 2021;13 (24):10748–10764. doi:10.1039/D1NR02065J
25. Bajracharya R, Song JG, Patil BR, et al. Functional ligands for improving anticancer drug therapy: current status and applications to drug delivery systems. *Drug Deliv*. 2022;29(1):1959–1970. doi:10.1080/10717544.2022.2089296
26. Yan S, Na J, Liu X, Wu P. Different targeting ligands-mediated drug delivery systems for tumor therapy. *Pharmaceutics*. 2024;16(2):248. doi:10.3390/pharmaceutics16020248
27. Chithrani BD, Ghazani AA, Chan WCW. Determining the size and shape dependence of gold nanoparticle uptake into mammalian cells. *Nano Lett*. 2006;6(4):662–668. doi:10.1021/nl052396o
28. Foroozandeh P, Aziz AA. Insight into cellular uptake and intracellular trafficking of nanoparticles. *Nanoscale Res Lett*. 2018;13(1):339. doi:10.1186/s11671-018-2728-6
29. Behzadi S, Serpooshan V, Tao W, et al. Cellular uptake of nanoparticles: journey inside the cell. *Chem Soc Rev*. 2017;46(14):4218–4244. doi:10.1039/C6CS00636A
30. Sousa De Almeida M, Susnik E, Drasler B, Taladriz-Blanco P, Petri-Fink A, Rothen-Rutishauser B. Understanding nanoparticle endocytosis to improve targeting strategies in nanomedicine. *Chem Soc Rev*. 2021;50(9):5397–5434. doi:10.1039/D0CS01127D
31. Zhang S, Gao H, Bao G. Physical principles of nanoparticle cellular endocytosis. *ACS Nano*. 2015;9(9):8655–8671. doi:10.1021/acsnano.5b03184
32. Augustine R, Hasan A, Primavera R, Wilson RJ, Thakor AS, Kevadiya BD. Cellular uptake and retention of nanoparticles: insights on particle properties and interaction with cellular components. *Mater Today Commun*. 2020;25:101692. doi:10.1016/j.mtcomm.2020.101692
33. Park JH, Oh N. Endocytosis and exocytosis of nanoparticles in mammalian cells. *Int J Nanomed*. 2014;51. doi:10.2147/IJN.S26592
34. Natarajan P, Tomich JM. Understanding the influence of experimental factors on bio-interactions of nanoparticles: towards improving correlation between in vitro and in vivo studies. *Arch Biochem Biophys*. 2020;694:108592. doi:10.1016/j.abb.2020.108592
35. Miao L, Huang L. Exploring the tumor microenvironment with nanoparticles. In: Mirkin CA, Meade TJ, Petrosko SH, Stegh AH editors, *Nanotechnology-Based Precision Tools for the Detection and Treatment of Cancer*. Vol. 166. Cancer Treatment and Research. Springer International Publishing; 2015:193–226. doi:10.1007/978-3-319-16555-4_9
36. Van Zundert I, Fortuni B, Rocha S. From 2D to 3D cancer cell models—the enigmas of drug delivery research. *Nanomaterials*. 2020;10 (11):2236. doi:10.3390/nano10112236
37. Rampado R, Crotti S, Caliceti P, Pucciarelli S, Agostini M. Recent advances in understanding the protein corona of nanoparticles and in the formulation of "stealthy" nanomaterials. *Front Bioeng Biotechnol*. 2020;8:166. doi:10.3389/fbioe.2020.00166
38. Chen F, Wang G, Griffin JI, et al. Complement proteins bind to nanoparticle protein corona and undergo dynamic exchange in vivo. *Nat Nanotechnol*. 2017;12(4):387–393. doi:10.1038/nnano.2016.269
39. Torrice M. Does nanomedicine have a delivery problem? *ACS Cent Sci*. 2016;2(7):434–437. doi:10.1021/acscentsci.6b00190
40. Fu XY, Yin H, Chen XT, et al. Three rounds of stability-guided optimization and systematical evaluation of oncolytic peptide LTX-315. *J Med Chem*. 2024;67(5):3885–3908. doi:10.1021/acs.jmedchem.3c02232
41. Qi YK, Zheng JS, Liu L. Mirror-image protein and peptide drug discovery through mirror-image phage display. *Chem*. 2024;10(8):2390–2407. doi:10.1016/j.chempr.2024.06.004
42. Mahmoudi M, Landry MP, Moore A, Coreas R. The protein corona from nanomedicine to environmental science. *Nat Rev Mater*. 2023;8 (7):422–438. doi:10.1038/s41578-023-00552-2
43. Zhang S, Chen W, Zhou J, et al. The benefits and safety of monoclonal antibodies: implications for cancer immunotherapy. *J Inflamm Res*. 2025;18:4335–4357. doi:10.2147/JIR.S499403
44. Miserocchi G, Bocchini M, Cortesi M, et al. Combining preclinical tools and models to unravel tumor complexity: jump into the next dimension. *Front Immunol*. 2023;14:1171141. doi:10.3389/fimmu.2023.1171141
45. Chithrani BD, Chan WCW. Elucidating the mechanism of cellular uptake and removal of protein-coated gold nanoparticles of different sizes and shapes. *Nano Lett*. 2007;7(6):1542–1550. doi:10.1021/nl070363y
46. Van Leent MMT, Priem B, Schrijver DP, et al. Regulating trained immunity with nanomedicine. *Nat Rev Mater*. 2022;7(6):465–481. doi:10.1038/s41578-021-00413-w

47. Agarwal R, Singh V, Jurney P, Shi L, Sreenivasan SV, Roy K. Mammalian cells preferentially internalize hydrogel nanodiscs over nanorods and use shape-specific uptake mechanisms. *Proc Natl Acad Sci*. 2013;110(43):17247–17252. doi:10.1073/pnas.1305000110
48. Jurney P, Agarwal R, Singh V, et al. Unique size and shape-dependent uptake behaviors of non-spherical nanoparticles by endothelial cells due to a shearing flow. *J Control Release*. 2017;245:170–176. doi:10.1016/j.jconrel.2016.11.033
49. Corbo C, Molinaro R, Parodi A, Toledano furman NE, Salvatore F, Tasciotti E. The impact of nanoparticle protein corona on cytotoxicity, immunotoxicity and target drug delivery. *Nanomed*. 2016;11(1):81–100. doi:10.2217/nnm.15.188
50. Tenzer S, Docter D, Kuharev J, et al. Rapid formation of plasma protein Corona critically affects nanoparticle pathophysiology. *Nat Nanotechnol*. 2013;8(10):772–781. doi:10.1038/nnano.2013.181
51. Yan Y, Gause KT, Kamphuis MMJ, et al. Differential roles of the protein corona in the cellular uptake of nanoporous polymer particles by monocyte and macrophage cell lines. *ACS Nano*. 2013;7(12):10960–10970. doi:10.1021/nn404481f
52. Neshatian M, Chung S, Yohan D, Yang C, Chithrani DB. Determining the size dependence of colloidal gold nanoparticle uptake in a tumor-like interface (Hypoxic). *Colloids Interface Sci Commun*. 2014;1:57–61. doi:10.1016/j.colcom.2014.07.004
53. Bromma K, Beckham W, Chithrani DB. Utilizing two-dimensional monolayer and three-dimensional spheroids to enhance radiotherapeutic potential by combining gold nanoparticles and docetaxel. *Cancer Nanotechnol*. 2023;14(1):80. doi:10.1186/s12645-023-00231-5
54. Yohan D, Cruje C, Lu X, Chithrani DB. Size-dependent gold nanoparticle interaction at nano–micro interface using both monolayer and multilayer (Tissue-Like) cell models. *Nano-Micro Lett*. 2016;8(1):44–53. doi:10.1007/s40820-015-0060-6
55. Yang C, Bromma K, Chithrani D. Peptide mediated in vivo tumor targeting of nanoparticles through optimization in single and multilayer in vitro cell models. *Cancers*. 2018;10(3):84. doi:10.3390/cancers10030084
56. Agarwal R, Jurney P, Raythatha M, et al. Effect of shape, size, and aspect ratio on nanoparticle penetration and distribution inside solid tissues using 3d spheroid models. *Adv Healthc Mater*. 2015;4(15):2269–2280. doi:10.1002/adhm.201500441
57. Tchoryk A, Taresco V, Argent RH, et al. Penetration and uptake of nanoparticles in 3D tumor spheroids. *Bioconjug Chem*. 2019;30 (5):1371–1384. doi:10.1021/acs.bioconjchem.9b00136
58. Zhu D, Brückner D, Sosniok M, et al. Size-dependent penetration depth of colloidal nanoparticles into cell spheroids. *Adv Drug Deliv Rev*. 2025;222:115593. doi:10.1016/j.addr.2025.115593
59. Cybulski P, Bravo M, Chen JJK, et al. Nanoparticle accumulation and penetration in 3D tumor models: the effect of size, shape, and surface charge. *Front Cell Dev Biol*. 2025;12:1520078. doi:10.3389/fcell.2024.1520078
60. Ahmed-Cox A, Pandzic E, Johnston ST, et al. Spatio-temporal analysis of nanoparticles in live tumor spheroids impacted by cell origin and density. *J Control Release*. 2022;341:661–675. doi:10.1016/j.jconrel.2021.12.014
61. Chen W, Wang W, Xie Z, et al. Size-dependent penetration of nanoparticles in tumor spheroids: a multidimensional and quantitative study of transcellular and paracellular pathways. *Small*. 2024;20(8):2304693. doi:10.1002/smll.202304693
62. Bromma K, Alhussan A, Perez MM, Howard P, Beckham W, Chithrani DB. Three-dimensional tumor spheroids as a tool for reliable investigation of combined gold nanoparticle and docetaxel treatment. *Cancers*. 2021;13(6):1465. doi:10.3390/cancers13061465
63. Bromma K, Dos Santos N, Barta I, et al. Enhancing nanoparticle accumulation in two dimensional, three dimensional, and xenograft mouse cancer cell models in the presence of docetaxel. *Sci Rep*. 2022;12(1):13508. doi:10.1038/s41598-022-17752-5
64. Wu J. The Enhanced Permeability and Retention (EPR) Effect: the significance of the concept and methods to enhance its application. *J Pers Med*. 2021;11(8):771. doi:10.3390/jpm11080771
65. Zhang YN, Poon W, Tavares AJ, McGilvray ID, Chan WCW. Nanoparticle–liver interactions: cellular uptake and hepatobiliary elimination. *J Control Release*. 2016;240:332–348. doi:10.1016/j.jconrel.2016.01.020
66. Puvanakrishnan P. In vivo tumor targeting of gold nanoparticles: effect of particle type and dosing strategy. *Int J Nanomed*. 2012;1251. doi:10.2147/IJN.S29147
67. Sykes EA, Dai Q, Sarsons CD, et al. Tailoring nanoparticle designs to target cancer based on tumor pathophysiology. *Proc Natl Acad Sci*. 2016;113(9). doi:10.1073/pnas.1521265113
68. Schädlich A, Caysa H, Mueller T, et al. Tumor accumulation of NIR fluorescent PEG–PLA nanoparticles: impact of particle size and human xenograft tumor model. *ACS Nano*. 2011;5(11):8710–8720. doi:10.1021/nn2026353
69. Yang H, He H, Tong Z, Xia H, Mao Z, Gao C. The impact of size and surface ligand of gold nanorods on liver cancer accumulation and photothermal therapy in the second near-infrared window. *J Colloid Interface Sci*. 2020;565:186–196. doi:10.1016/j.jcis.2020.01.026
70. De Jong WH, Hagens WI, Krystek P, Burger MC, Ajam S, Geertsma RE. Particle size-dependent organ distribution of gold nanoparticles after intravenous administration. *Biomaterials*. 2008;29(12):1912–1919. doi:10.1016/j.biomaterials.2007.12.037
71. Soo Choi H, Liu W, Misra P, et al. Renal clearance of quantum dots. *Nat Biotechnol*. 2007;25(10):1165–1170. doi:10.1038/nbt1340
72. Longmire M, Choyke PL, Kobayashi H. Clearance properties of nano-sized particles and molecules as imaging agents: considerations and caveats. *Nanomed*. 2008;3(5):703–717. doi:10.2217/17435889.3.5.703
73. Cecchi D, Niddrie M, Freeman S, et al. Route of administration of functionalized gold nanoparticles improves tumor accumulation in vivo. *ACS Appl Nano Mater*. 2025;8(46):22308–22319. doi:10.1021/acsanm.5c04161
74. Jasinski DL, Li H, Guo P. The effect of size and shape of RNA nanoparticles on biodistribution. *Mol Ther*. 2018;26(3):784–792. doi:10.1016/j.ymthe.2017.12.018
75. Blanco E, Shen H, Ferrari M. Principles of nanoparticle design for overcoming biological barriers to drug delivery. *Nat Biotechnol*. 2015;33 (9):941–951. doi:10.1038/nbt.3330
76. Albanese A, Tang PS, Chan WCW. The effect of nanoparticle size, shape, and surface chemistry on biological systems. *Annu Rev Biomed Eng*. 2012;14(1):1–16. doi:10.1146/annurev-bioeng-071811-150124
77. Jain RK, Stylianopoulos T. Delivering nanomedicine to solid tumors. *Nat Rev Clin Oncol*. 2010;7(11):653–664. doi:10.1038/nrclinonc.2010.139
78. Jain RK. Transport of molecules in the tumor interstitium: a review. *Cancer Res*. 1987;47(12):3039–3051.
79. Hobbs SK, Monsky WL, Yuan F, et al. Regulation of transport pathways in tumor vessels: role of tumor type and microenvironment. *Proc Natl Acad Sci*. 1998;95(8):4607–4612. doi:10.1073/pnas.95.8.4607
80. Heldin CH, Rubin K, Pietras K, Östman A. High interstitial fluid pressure — an obstacle in cancer therapy. *Nat Rev Cancer*. 2004;4 (10):806–813. doi:10.1038/nrc1456

81. Wilhelm S, Tavares AJ, Dai Q, et al. Analysis of nanoparticle delivery to tumours. *Nat Rev Mater*. 2016;1(5):16014. doi:10.1038/natrevmats.2016.14
82. Dobrovolskaia MA, Aggarwal P, Hall JB, McNeil SE. Preclinical studies to understand nanoparticle interaction with the immune system and its potential effects on nanoparticle biodistribution. *Mol Pharm*. 2008;5(4):487–495. doi:10.1021/mp800032f
83. Salvati A, Pitek AS, Monopoli MP, et al. Transferrin-functionalized nanoparticles lose their targeting capabilities when a biomolecule Corona adsorbs on the surface. *Nat Nanotechnol*. 2013;8(2):137–143. doi:10.1038/nnano.2012.237
84. Bertrand N, Grenier P, Mahmoudi M, et al. Mechanistic understanding of in vivo protein Corona formation on polymeric nanoparticles and impact on pharmacokinetics. *Nat Commun*. 2017;8(1):777. doi:10.1038/s41467-017-00600-w
85. Talamini L, Violatto MB, Cai Q, et al. Influence of size and shape on the anatomical distribution of endotoxin-free gold nanoparticles. *ACS Nano*. 2017;11(6):5519–5529. doi:10.1021/acsnano.7b00497
86. Poon W, Zhang X, Bekah D, Teodoro JG, Nadeau JL. Targeting B16 tumors *in vivo* with peptide-conjugated gold nanoparticles. *Nanotechnology*. 2015;26(28):285101. doi:10.1088/0957-4484/26/28/285101
87. Braun GB, Sugahara KN, Yu OM, et al. Urokinase-controlled tumor penetrating peptide. *J Control Release*. 2016;232:188–195. doi:10.1016/j.jconrel.2016.04.027
88. Jackson N, Morgan J, Valath A, et al. Effects of docetaxel and host immune status on nanoparticle biodistribution and tumor uptake. *ACS Appl Nano Mater*. 2025;8(1):210–222. doi:10.1021/acsanm.4c05460
89. Jackson N, Bouzeineddine N, Cecchi D, et al. Comprehensive analysis of the tumor targeting efficiency of functionalized nanoparticles in an immunocompetent environment. *Sci Rep*. 2025;15(1):35225. doi:10.1038/s41598-025-22151-7
90. Iureva AM, Nikitin PI, Tereshina ED, Nikitin MP, Shipunova VO. The influence of various polymer coatings on the in vitro and in vivo properties of PLGA nanoparticles: comprehensive study. *Eur J Pharm Biopharm*. 2024;201:114366. doi:10.1016/j.ejpb.2024.114366
91. Yu T, Greish K, McGill LD, Ray A, Ghandehari H. Influence of geometry, porosity, and surface characteristics of silica nanoparticles on acute toxicity: their vasculature effect and tolerance threshold. *ACS Nano*. 2012;6(3):2289–2301. doi:10.1021/nn2043803
92. Yu T, Hubbard D, Ray A, Ghandehari H. In vivo biodistribution and pharmacokinetics of silica nanoparticles as a function of geometry, porosity and surface characteristics. *J Control Release*. 2012;163(1):46–54. doi:10.1016/j.jconrel.2012.05.046
93. Wei D, Pang K, Song Q, et al. Noninvasive monitoring of nanoparticle clearance and aggregation in blood circulation by in vivo flow cytometry. *J Control Release*. 2018;278:66–73. doi:10.1016/j.jconrel.2018.03.024
94. Bai X, Wang J, Mu Q, Su G. In vivo protein corona formation: characterizations, effects on engineered nanoparticles' biobehaviors, and applications. *Front Bioeng Biotechnol*. 2021;9:646708. doi:10.3389/fbioe.2021.646708
95. Simon J, Kuhn G, Fichter M, Gehring S, Landfester K, Mailänder V. Unraveling the in vivo protein corona. *Cells*. 2021;10(1):132. doi:10.3390/cells10010132
96. Yaremenko AV, Zelepukin IV, Ivanov IN, et al. Influence of magnetic nanoparticle biotransformation on contrasting efficiency and iron metabolism. *J Nanobiotechnology*. 2022;20(1):535. doi:10.1186/s12951-022-01742-w
97. Dai Q, Wilhelm S, Ding D, et al. Quantifying the ligand-coated nanoparticle delivery to cancer cells in solid tumors. *ACS Nano*. 2018;12(8):8423–8435. doi:10.1021/acsnano.8b03900
98. Miller MA, Zheng YR, Gadde S, et al. Tumour-associated macrophages act as a slow-release reservoir of nano-therapeutic Pt(IV) pro-drug. *Nat Commun*. 2015;6(1):8692. doi:10.1038/ncomms9692
99. Hare JI, Lammers T, Ashford MB, Puri S, Storm G, Barry ST. Challenges and strategies in anti-cancer nanomedicine development: an industry perspective. *Adv Drug Deliv Rev*. 2017;108:25–38. doi:10.1016/j.addr.2016.04.025
100. Guerin MV, Finisguerra V, Van Den Eynde BJ, Bercovici N, Trautmann A. Preclinical murine tumor models: a structural and functional perspective. *eLife*. 2020;9:e50740. doi:10.7554/eLife.50740
101. Siemann DW. The unique characteristics of tumor vasculature and preclinical evidence for its selective disruption by tumor-vascular disrupting agents. *Cancer Treat Rev*. 2011;37(1):63–74. doi:10.1016/j.ctrv.2010.05.001
102. Shi J, Kantoff PW, Wooster R, Farokhzad OC. Cancer nanomedicine: progress, challenges and opportunities. *Nat Rev Cancer*. 2017;17(1):20–37. doi:10.1038/nrc.2016.108